Enhanced Open-Circuit Voltage in Colloidal Quantum Dot Photovoltaics via Reactivity-Controlled Solution-Phase Ligand Exchange

Jea Woong Jo, Younghoon Kim, Jongmin Choi, F. Pelayo García de Arquer, Grant Walters, Bin Sun, Olivier Ouellette, Junghwan Kim, Andrew H. Proppe, Rafael Quintero-Bermudez, James Fan, Jixian Xu, Chih Shan Tan, Oleksandr Voznyy,* and Edward H. Sargent*

The energy disorder that arises from colloidal quantum dot (CQD) polydispersity limits the open-circuit voltage (V_{OC}) and efficiency of CQD photovoltaics. This energy broadening is significantly deteriorated today during CQD ligand exchange and film assembly. Here, a new solution-phase ligand exchange that, via judicious incorporation of reactivity-engineered additives, provides improved monodispersity in final CQD films is reported. It has been found that increasing the concentration of the less reactive species prevents CQD fusion and etching. As a result, CQD solar cells with a V_{OC} of 0.7 V (vs 0.61 V for the control) for CQD films with exciton peak at 1.28 eV and a power conversion efficiency of 10.9% (vs 10.1% for the control) is achieved.

Colloidal quantum dots (CQDs) are quantum-confined nanocrystals widely explored for use in optoelectronic applications, such as light-emitting diodes,[1,2] lasers,[3] transistors,[4,5] and photodetectors.[6,7] Metal chalcogenide CQDs have attracted interest as a promising photoactive material for solution-processed photovoltaics (PVs) by virtue of their bandgap tunable across the solar spectrum.[8–10] Intensive research during the past decade has led to advances in high-quality CQDs and in preserving these characteristics from solution into film. Efforts to improve synthesis, ligand exchange and passivation, interface engineering, and device fabrication have led to photovoltaic performance enhancements[11–15] and a recent record certified power conversion efficiency (PCE) of 11.3%. This latest advance came from replacing the legacy tetrabutylammonium (TBA) iodide layer-by-layer ligand exchange with a halide-based solution-phase ligand exchange.[16] The performance increase stemmed from a major improvement in CQD passivation and monodispersity.

There remains a large energy loss beyond the Shockley–Queisser limit ($E_{loss} = qV_{SQ} - qV_{OC}$, where V_{SQ} is the Shockley–Queisser limit of open-circuit voltage for a given bandgap, defined as a center of the exciton peak in CQD films, q is the elementary charge, and V_{OC} is the open-circuit voltage), resulting in the V_{OC} deficit, which is a critical factor that curtails CQD photovoltaic performance. The E_{loss} observed in highly efficient inorganic and perovskite solar cells is in the range of 0.1–0.2 eV and stems from trap recombination losses that drain the carrier population and thus reduce V_{OC}.[17,18] However, the E_{loss} in CQD photovoltaics can reach fully 0.4 eV. It arises not from increased recombination losses but rather from the difference between the exciton peak position and the true bandedge, since photocarriers quickly thermalize to the lowest energy bandtails. The best reported E_{loss} has been lowered to 0.31 eV, but at the expense of reduced J_{SC}. These considerations indicate that there remains considerable room for V_{OC} enhancement.[12,19–21]

The energy disorder arising from CQD polydispersity is a major reason behind the large E_{loss}, for it causes bandtail broadening.[22–24] Different synthetic routes have been explored seeking to obtain more energetically homogeneous CQD solids.[25–28] However, the ligand exchange process itself is one of the major contributors to energetic disorder in CQD solids and up to a ≈50% increase in polydispersity is produced therein.[16] The substitution of the long insulating (i.e., oleic acid (OA)) ligands (used for synthesis) by the short conductive ligands (needed for carrier transport) is accompanied by surface stripping that leads to nanocrystal fusion.[29,30]

Here, we report a new solution-phase ligand exchange that exploits the combination of two chemical reagents with different reactivities. They simultaneously provide passivation, CQD assembly, and charge transport while preserving the homogeneity of the CQD population. In particular, we employ a mixture of ammonium acetate (AA) and tetrabutylammonium acetate (TBAA), and correlate the reactivity during the ligand exchange with the homogeneity of resulting CQD films. From this, we achieve CQD solar cells that exhibit a low E_{loss}
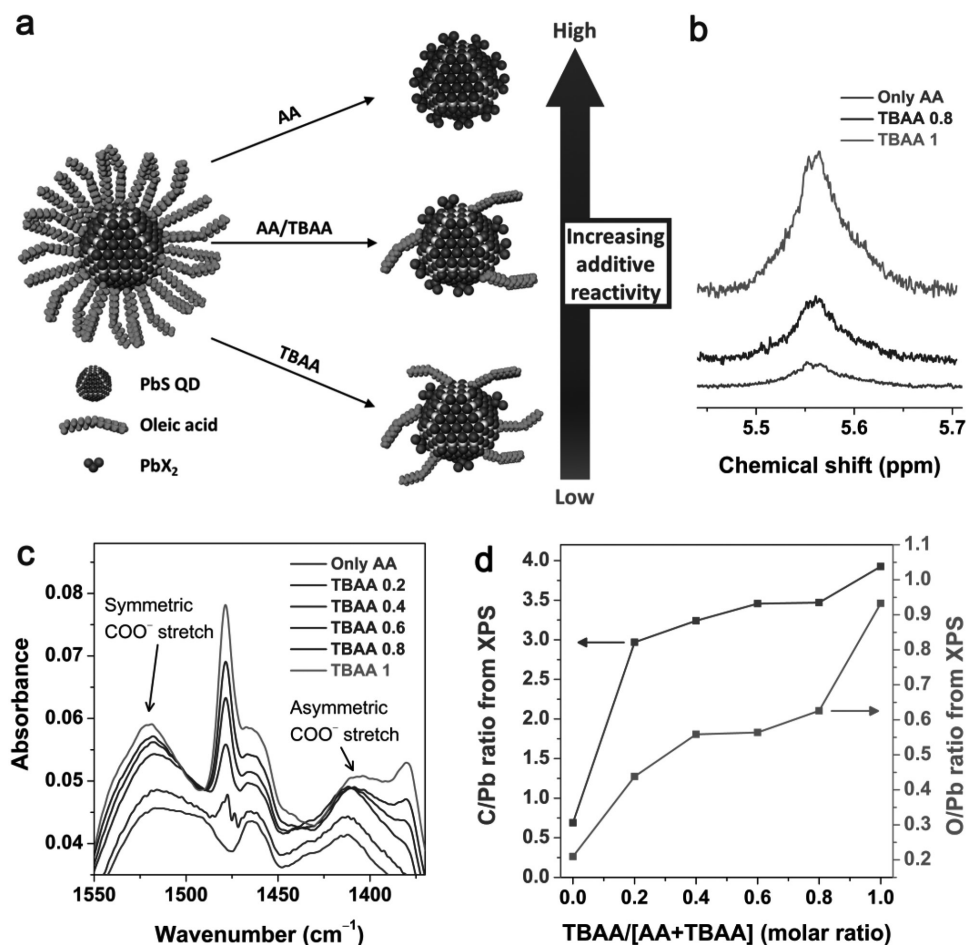
Dr. J. W. Jo, Dr. Y. Kim,[+] Dr. J. Choi, Dr. F. P. G. de Arquer, G. Walters, Dr. B. Sun, O. Ouellette, Dr. J. Kim, A. H. Proppe, R. Quintero-Bermudez, J. Fan, Dr. J. Xu, Dr. C. S. Tan, Dr. O. Voznyy, Prof. E. H. Sargent
Department of Electrical and Computer Engineering
University of Toronto
10 King's College Road, Toronto, Ontario M5S 3G4, Canada
E-mail: o.voznyy@utoronto.ca; ted.sargent@utoronto.ca
[+]Present address: Convergence Research Center for Solar Energy, Daegu Gyeongbuk Institute of Science and Technology, Daegu 42988, Republic of Korea

1703627 (1 of 6)

ADVANCED
SCIENCE NEWS
www.advancedsciencenews.com

ADVANCED
MATERIALS
www.advmat.de

Figure 1. Reactivity control during solution-phase ligand exchange of CQDs. a) Schematic illustration of the control by mixing AA and TBAA reagents. b) ^{1}H NMR spectra of CQDs after solution-phase ligand exchange with different AA/TBAA blend ratios. c) FT-IR spectra of CQD films prepared using different blend ratios of AA/TBAA. d) C/Pb and O/Pb ratios calculated from XPS spectra of CQD films prepared using different AA/TBAA ratios.

of 0.31 eV, a record (for CQD photovoltaic) V_{OC} of 0.7 V, and a high PCE of 10.9% compared to 10.1% reference samples.

We took the view that preserving trace amounts of OA on the CQD surfaces during ligand exchange could help avoid quantum dot fusion and etching. This could ultimately lead to reduced energetic disorder (**Figure 1**a).[29] We hypothesized that by selectively including reagents that exhibit different reactivity toward the CQD surface, we could then tune the overall kinetics of the ligand exchange reaction.[31,32]

To test our hypothesis, we included AA and TBAA reagents during the halide-based solution-phase ligand exchange. We selected TBAA in view of the lower reactivity of the TBA$^+$ counterion toward OA displacement compared to the ammonium, a result of less acidic character of TBA,[31] leading to milder reaction conditions that would help preserve OA ligands. We studied different blend ratios of AA:TBAA = 1:0, 0.8:0.2, 0.6:0.4, 0.4:0.6, 0.2:0.8, and 0:1, which for brevity we denote AA, TBAA 0.2, TBAA 0.4, TBAA 0.6, TBAA 0.8, and TBAA 1, respectively.

The chemical structure of CQD inks after ligand exchange was investigated using ^{1}H NMR spectroscopy (Figure 1b). In all samples, the signal associated with the proton on the C=C bond of OA was observed between 5.5–5.6 ppm. This indicates

that OA ligands remain in all CQD inks following ligand exchange reactions. The calibrated intensities using the NMR signal from n-butylamine (BTA) revealed an increase in the amount of OA present in the ink when the relative concentration of TBAA increases (Figure S1, Supporting Information). The NMR signals associated with TBAA remained below detection limit, suggesting that most of TBAA is removed during ligand exchange process (washing, precipitation, and drying under vacuum).

To further identify the influence of different AA/TBAA blend ratios on the CQD chemical composition, we prepared CQD films from the resulting inks, where a BTA: dimethylformamide (DMF) (20:1 v/v) solution was used to redisperse the ligand-exchanged CQDs. Fourier transform infrared spectroscopy (FT-IR) further confirms this finding, showing an increased presence of OA vibrational modes as the ratio of TBAA increased (Figure 1c and Figure S2, Supporting Information). C/Pb and O/Pb ratios in CQD films obtained from X-ray photoelectron spectroscopy (XPS) measurements also show a similar trend (Figure 1d and Table S1, Supporting Information). From these results, we confirm that the ligand exchange reaction can be controlled by changing the relative ratio of
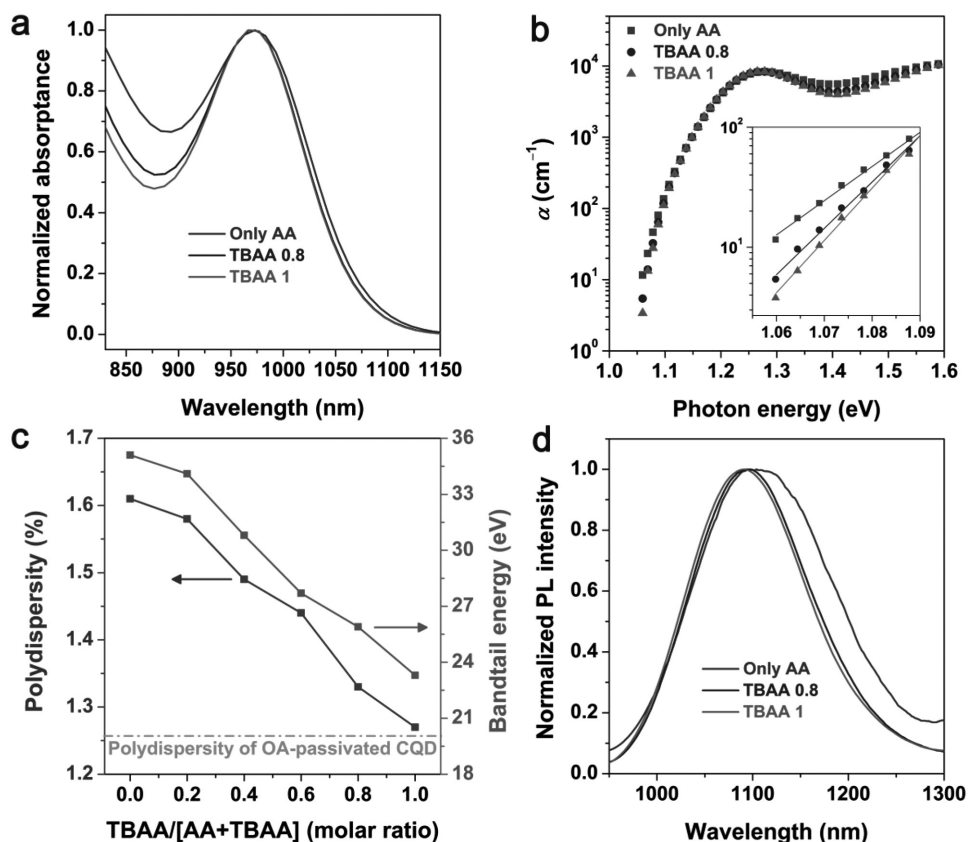
Figure 2. The effects of AA/TBAA ratio on polydispersity and bandtails of CQD films. a) Normalized optical absorptance of CQD films after solution-phase ligand exchange using different AA/TBAA blend ratios. b) Absorption coefficient measured by photothermal deflection spectroscopy for different CQD films. c) Polydispersity and bandtail energy of CQD films as a function of TBAA/[AA+TBAA] ratio. d) Normalized PL spectra of CQD films prepared using different blend ratios of AA/TBAA.

AA/TBAA, and that the fraction of OA remaining after ligand exchange monotonically increases with TBAA content.

The homogeneity of CQD films prepared with different ratios of AA/TBAA was compared by performing UV–vis absorption spectroscopy (**Figure 2**a and Figure S4a, Supporting Information). The films showed an almost identical exciton peak position; however, a narrower peak with a lower full-width at half-maximum (FWHM) was observed as the TBAA ratio increased. Higher absorption at 900 nm is a consequence of excitonic peak broadening that is also responsible for wider bandtails.

To characterize the degree of energetic disorder of CQD films in detail, we extracted the polydispersity and bandtail energy from the FWHM of optical absorption spectra (Figure S4b, Supporting Information) and the absorption coefficient of the different films using photothermal deflection spectroscopy (Figure 2b).[16,24,27,33] Notably, the polydispersity of the CQD films was significantly reduced from 1.61% for AA to 1.58%, 1.49%, 1.44%, 1.33%, and 1.27% as the TBAA ratio varies from 0.2, 0.4, 0.6, 0.8, and 1, respectively (Figure 2c). The polydispersity of TBAA ratio 1 was very close to the value of OA-passivated CQDs before ligand exchange (1.26%). The energy landscape of CQD films was found to be flatter as the TBAA ratio increases. The CQD bandtail sharpens and the associated bandtail energy decreases from 35.1 to 23.3 meV (Figure S5,

Supporting Information), which we ascribe to a reduction in inhomogeneous necking of CQDs. The improved homogeneity of CQD TBAA/AA ligand-exchanged films is further supported by photoluminescence (PL) analysis of the films: a PL spectrum with a reduced FWHM was obtained for increasing TBAA concentration, indicative of decreasing carrier funneling (Figure 2d and Figure S6c, Supporting Information). The PL intensity was enhanced in films when we increased the amount of TBAA, a fact we assign to slower exciton dissociation and slower transport-assisted trap recombination in films that contain the higher amount of insulating OA ligands (Figure S6a, Supporting Information).

We then sought to investigate how the increased homogeneity of the CQD films obtained using the TBAA/AA-controlled halide ligand exchange translates into the photovoltaic properties of CQD solar cells. We fabricated solar cells consisting of indium tin oxide (ITO)/zinc oxide (ZnO)/lead halide-passivated CQD/1,2-ethanedithiol (EDT)-treated CQD/Au and characterized the devices a function of TBAA amount (Figure S8, Supporting Information). All CQD photovoltaics showed good air stability, retaining more than 95% of their initial PCE following 120 h of storage in air (Figure S10, Supporting Information).

We observed that the V_{OC} consistently increased for increasing TBAA ratio, from an average value of 0.61–0.70 V as TBAA increased from 0 to 1. This corresponds to a decreasing
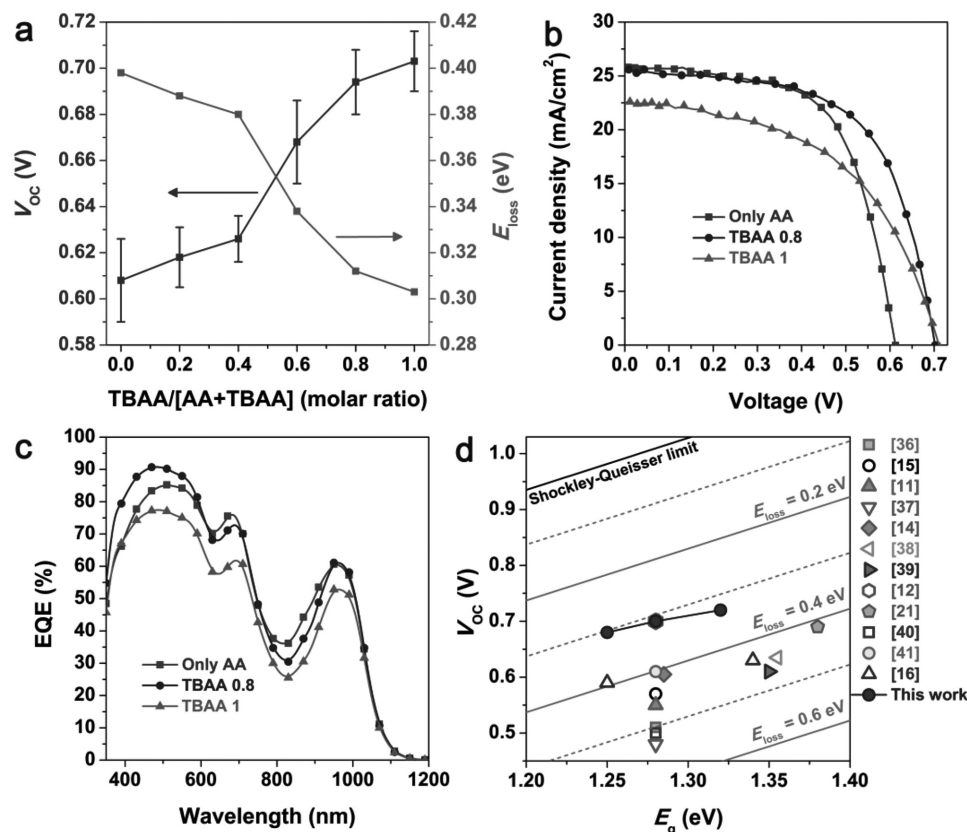
**ADVANCED
SCIENCE NEWS**

www.advancedsciencenews.com

**ADVANCED
MATERIALS**

www.advmat.de

Figure 3. V_{OC} enhancement in CQD photovoltaics prepared using AA/TBAA blend. a) V_{OC} and E_{loss} change of CQD photovoltaics as a function of TBAA/[AA+TBAA] ratio. b) J–V curves and c) EQE spectra of CQD photovoltaics prepared using three different blending ratios (AA: TBAA = 1:0, 0.2:0.8, and 0:1). d) Comparison of E_{loss} values of CQD photovoltaics prepared using reactivity control with other CQD photovoltaics reported in the literature. For the calculation of E_{loss}, the bandgap (E_g) is measured from exciton peak center.

E_{loss} (0.40–0.30 eV) (**Figure 3**a) and is consistent with reduced bandtails seen in high dynamic range external quantum efficiency (HDR EQE) measurements (Figure S9, Supporting Information). A notable decrease was observed in the short-circuit current (J_{SC}) for TBAA 1, even though the device thickness and absorbance are comparable to other samples (Figure S7, Supporting Information). Similarly, the fill factor (FF) of the devices was maintained up to a TBAA ratio of 0.8, but dropped sharply for the highest concentration. The V_{OC}–J_{SC} compromise is typical for devices with reduced mobility which in this case is due to increased amounts of insulating ligands. Lower mobility leads to increased accumulation of carriers and this triggers enhanced radiative recombination losses;[29,34,35] however, in controlled amounts, it can be beneficial for enhanced quasi-Fermi level splitting, positively affecting the V_{OC}. We show below that a controlled reduction of the amount of TBAA, and thus of the remnant OA in the film, allows us to avoid the V_{OC}–J_{SC} compromise. The highest device performance was observed for TBAA 0.8 with a high PCE of 10.9%, a V_{OC} of 0.70 V, a J_{SC} of 25.3 mA cm^{-2}, and an FF of 62% (Figure 3b and **Table 1**). In contrast, reference samples using only AA showed a PCE of 10.1%, with a V_{OC} of 0.61 V, a J_{SC} of 25.7 mA cm^{-2}, and an FF of 64%. The CQD devices showed an overall PCE slightly lower than best published results because a thinner photoactive layer (≈300 nm) was used to avoid film cracking

of films with high TBAA ratios upon the deposition of EDT-treated CQD layer.[16] We believe that the efficiency of CQD PV using the reactivity-controlled ligand exchange can be further improved by modification of the film deposition method or the hole transporting layer (i.e., EDT-CQD layer).

Comparison of the V_{OC} for our best device (TBAA 0.8) with other reported data for CQD photovoltaics shows the reduced energy loss (Figure 3d and Table S2, Supporting Information).[11,12,14–16,18,36–41] The AA/TBAA method shows a significantly improved V_{OC} for the CQDs with a bandgap in the range 1.25–1.32 eV (counting from the exciton peak in CQD films). TBAA 0.8 devices provided extremely small E_{loss} values ranging

Table 1. Device properties of CQD photovoltaics prepared using solution-phase ligand exchanges with three different blend ratios of AA/TBAA under standard AM 1.5 G illumination.

AA:TBAA	V_{OC} [V]	J_{SC} [mA cm^{-2}]	FF [%]	PCE$_{avg}$[a] [%]
1:0	0.61 ± 0.02	25.6 ± 0.8 (26.0[b])	62.0 ± 3.0	9.7 ± 0.4
0.2:0.8	0.69 ± 0.01	24.8 ± 0.7 (25.9[b])	61.1 ± 1.5	10.5 ± 0.4
0:1	0.70 ± 0.01	22.6 ± 0.7 (22.1[b])	45.9 ± 0.5	7.7 ± 0.3

[a]The averaged values calculated from at least eight devices; [b]Integrated from EQE data.

**ADVANCED
SCIENCE NEWS**

www.advancedsciencenews.com

**ADVANCED
MATERIALS**

www.advmat.de

between 0.30 and 0.33 eV. It should be noted that if counted from EQE bandedge, i.e., considering only the energy loss due to trap recombination, these numbers reduce to 0.13 eV (for CQDs with exciton peak center at 1.28 eV, EQE bandedge is at 1.08 eV and the Shockley–Queisser limit value for this bandgap is 0.83 V), approaching the values of crystalline silicon and perovskite solar cells (E_{loss} = 0.1–0.2 eV).

In summary, we developed a modified solution-phase ligand exchange method based on the tunable reactivity of AA/TBAA mixed reagents that leads to an improved monodispersity in CQD films. We found that increasing the concentration of the less reactive TBAA additive during halide ligand exchange leads to a controllable amount of OA remaining on the surface of CQDs. This militates against the CQD fusion and etching that increase inhomogeneity. As a result, we achieve CQD solar cells with a PCE increase caused by a significant increase in V_{OC} and a lowered E_{loss}. The optimized device (TBAA 0.8) shows a high PCE of 10.9% with an impressive V_{OC} of 0.7 V (E_{loss} = 0.31 eV) compared to a PCE of 10.1% and a V_{OC} of 0.61 V in reference samples with the same exciton peak position. Our approach adds more degrees of freedom in the control over CQD ligand exchange that, by minimizing CQD polydispersity, can be leveraged to increase further the performance of CQD optoelectronic devices.

Experimental Section

Lead Halide Ligand Exchange of lead sulfide (PbS) CQDs: OA-passivated CQDs were synthesized by following previously reported method.[11] To lead iodide (1.50 mmol, 0.691 mg) and lead bromide (0.33 mmol, 0.121 mg) in DMF (5 mL), AA and TBAA blends (0.62 mmol) were added. And then, 35 mg of OA-passivated CQDs (6 mg mL^{-1} in octane) were added. After phase transfer from octane to DMF by mixing vigorously for 2 min, the CQD solution in DMF was washed three times with octane. The ligand-exchanged CQDs were collected by precipitating with the addition of acetone (6 mL) and drying under vacuum for 20 min.

Characterization: ^{1}H NMR (Bruker Avance III 400) was carried out by using a mixture of BTA:DMF-d7 (0.015:1 v/v) as a solvent and tetramethylsilane as an internal reference material. FT-IR spectra were measured by FT-IR spectrometer (Bruker Tensor 27). XPS measurements (Thermo Scientific K-Alpha system) were performed using an Al Kα source. The optical absorption spectra were obtained by an UV–vis–IR spectrophotometer (Lambda 950). Photoluminescence was characterized by performing PL spectrophotometer (Ocean Optics NIR-512. The polydispersities of CQDs were extracted from the FWHM of optical absorption spectra by using previously reported equation[27]: FWHM (d, σ) = 2 σ (0.00543 d σ + 0.923 d + 1.34)/[(0.0118 σ + 1) (0.0392 d + 0.114)(0.000461 d σ + 0.0392 d + 0.114)d], where d and σ are the mean diameter and the polydispersity of CQD, respectively. The homogeneous linewidth for PbS single dots is reported to be ≈100 meV.[42] The real dispersities of CQD films were obtained by deducting homogenous linewidths from FWHM of CQD ensembles.[16]

Device Fabrication and Testing: CQD photovoltaics were prepared with a device configuration of ITO/ZnO/lead halide passivated PbS CQD/EDT treated PbS CQD/Au. ZnO nanoparticles were synthesized by following the methods in previously reported paper.[20] The ZnO nanoparticle solution was spin-coated two times on the ITO-coated glass at 3000 rpm for 30 s. Then, lead halide passivated PbS CQD solution (200–250 mg mL^{-1} in 20:1 (v/v) BTA:DMF) were spin coated at 2500 rpm for 30 s. Two layers of EDT-treated CQDs were deposited on the top of each CQD film by following reported method.[20] Finally, Au (120 nm) was thermally evaporated under vacuum (<10^{-6} Torr). The effective area of device was 0.049 cm^2. The *J*–*V* characteristics of CQD

photovoltaics were measured using a Keithley 2400 source-meter. The simulated AM 1.5 G illumination (Sciencetech class 3A) was obtained with an Xe lamp and filters (Solar Light Company Inc.), and the light intensity (100 mW cm^{-2}) was calibrated with a reference Si solar cell (Newport, Inc.). EQE spectra were measured under monochromatic illumination (400 W Xe lamp equipped with a monochromator and cutoff filters). Newport 818-UV and Newport 838-IR photodetectors were utilized for calibration. The current response was collected at short-circuit conditions with a Lakeshore preamplifier connected to a Stanford Research 830 lock-in amplifier. The reliability of J_{SC} in *J*–*V* measurement was verified by comparing with J_{SC} values integrated from measured EQE spectra (Figure 3c and Table 1). HDR EQE was measured by adjusting the sensitivity of the preamplifier to 1 nA V^{-1}, providing the sufficient resolution of the EQEs at the infrared region >1100 nm. HDR EQE has been known to be able to detect the carrier density within bandtails due to high sensitivity and sharp slope of the linear region in HDR EQE represents the reduction of bandtail energy.[16,43,44] Cross-sectional images of the devices were investigated using the field-emission scanning electron microscope (Hitachi SU8230).

Supporting Information

Supporting Information is available from the Wiley Online Library or from the author.

Conflict of Interest

The authors declare no conflict of interest.

[1] V. L. Colvin, M. C. Schlamp, A. P. Alivisatos, *Nature* **1994**, *370*, 354.

[2] Q. J. Sun, Y. A. Wang, L. S. Li, D. Y. Wang, T. Zhu, C. H. Yang, Y. F. Li, *Nat. Photonics* **2007**, *1*, 717.

[3] V. I. Klimov, S. A. Ivanov, J. Nanda, M. Achermann, I. Bezel, J. A. McGuire, A. Piryatinski, *Nature* **2007**, *447*, 441.

[4] A. T. Fafarman, W.-K. Koh, B. T. Diroll, D. K. Kim, D.-K. Ko, S. J. Oh, X. Ye, V. Doan-Nguyen, M. R. Crump, D. C. Reifsnyder, C. B. Murray, C. R. Kagan, *J. Am. Chem. Soc.* **2011**, *133*, 15753.

[5] M. V. Kovalenko, M. Scheele, D. V. Talapin, *Science* **2009**, *324*, 1417.

[6] G. Konstantatos, I. Howard, A. Fischer, S. Hoogland, J. Clifford, E. Klem, L. Levina, E. H. Sargent, *Nature* **2006**, *442*, 180.

[7] J.-S. Lee, M. V. Kovalenko, J. Huang, D. S. Chung, D. V. Talapin, *Nat. Nanotechnol.* **2011**, *6*, 348.

[8] Z. Ning, O. Voznyy, J. Pan, S. Hoogland, V. Adinolfi, J. Xu, M. Li, A. R. Kirmani, J. Sun, J. Minor, K. W. Kemp, H. Dong, L. Rollny, A. Labelle, G. Carey, B. R. Sutherland, I. Hill, A. Amassian, H. Liu, J. Tang, O. M. Bakr, E. H. Sargent, *Nat. Mater.* **2014**, *13*, 822.

[9] Y. Kim, K. Bicanic, H. Tan, O. Ouellette, B. R. Sutherland, F. P. García de Arquer, J. W. Jo, M. Liu, B. Sun, M. Liu, S. Hoogland, E. H. Sargent, *Nano Lett.* **2017**, *17*, 2349.

[10] I. J. Kramer, E. H. Sargent, *Chem. Rev.* **2014**, *114*, 863.

[11] Z. Ning, D. Zhitomirsky, V. Adinolfi, B. R. Sutherland, J. Xu, O. Voznyy, P. Maraghechi, X. Lan, S. Hoogland, Y. Ren, E. H. Sargent. *Adv. Mater.* **2013**, *25*, 1719.

[12] A. K. Rath, F. P. García de Arquer, A. Stavrinadis, T. Lasanta, M. Bernechea, S. L. Diedenhofen, G. Konstantatos, *Adv. Mater.* **2014**, *26*, 4741.

[13] J. Tang, K. Y. Kemp, S. Hoogland, K. S. Jeong, H. Liu, L. Levina, M. Furukawa, X. Wang, R. Debnath, D. Cha, K. W. Chou, A. Fischer, A. Amassian, J. B. Asbury, E. H. Sargent, *Nat. Mater.* **2011**, *10*, 765.

[14] A. H. Ip, S. M. Thon, S. Hoogland, O. Voznyy, D. Zhitomirsky, R. Debnath, L. Levina, L. R. Rollny, G. H. Carey, A. Fischer, K. W. Kemp, I. J. Kramer, Z. Ning, A. J. Labelle, K. W. Chou, A. Amassian, E. H. Sargent, *Nat. Nanotechnol.* **2012**, *7*, 577.

[15] M. Yuan, D. Zhitomirsky, V. Adinolfi, O. Voznyy, K. W. Kemp, Z. Ning, X. Lan, J. Xu, J. Y. Kim, H. Dong, E. H. Sargent. *Adv. Mater.* **2013**, *25*, 5586.

[16] M. Liu, O. Voznyy, R. Sabatini, F. P. García de Arquer, R. Munir, A. H. Balawi, X. Lan, F. Fan, G. Walters, A. R. Kirmani, S. Hoogland, F. Laquai, A. Amassian, E. H. Sargent, *Nat. Mater.* **2017**, *16*, 258.

[17] C.-H. M. Chuang, A. Maurano, R. E. Brandt, G. W. Hwang, J. Jean, T. Buonassisi, V. Bulović, M. G. Bawendi, *Nano Lett.* **2015**, *15*, 3286.

[18] A. Polman, M. Knight, E. C. Garnett, B. Ehrler, W. C. Sinke, *Science* **2016**, *352*, aad4424.

[19] W. Yoon, J. E. Boercker, M. P. Lumb, D. Placencia, E. E. Foos, J. G. Tischler, *Sci. Rep.* **2013**, *3*, 2225.

[20] C.-H. M. Chuang, P. R. Brown, V. Bulović, M. G. Bawendi, *Nat. Mater.* **2014**, *13*, 796.

[21] S. Pradhan, A. Stavrinadis, S. Gupta, S. Christodoulou, G. Konstantatos, *ACS Energy Lett.* **2017**, *2*, 1444.

[22] P. T. Erslev, H.-Y. Chen, J. Gao, M. C. Beard, A. J. Frank, J. van de Lagemaat, J. C. Johnson, J. M. Luther, *Phys. Rev. B* **2012**, *86*, 155313.

[23] Y. Gao, E. Talgorn, M. Aerts, M. T. Trinh, J. M. Schins, A. J. Houtepen, L. D. A. Siebbeles, *Nano Lett.* **2011**, *11*, 5471.

[24] P. Guyot-Sionnest, *J. Phys. Chem. Lett.* **2012**, *3*, 1169.

[25] M. P. Hendricks, M. P. Campos, G. T. Cleveland, I. J.-L. Plante, J. S. Owen, *Science* **2015**, *348*, 1226.

[26] H. Choi, J.-H. Ko, Y.-H. Kim, S. Jeong, *J. Am. Chem. Soc.* **2013**, *135*, 5278.

[27] M. C. Weidman, M. E. Beck, R. S. Hoffman, F. Prins, W. A. Tisdale, *ACS Nano* **2014**, *8*, 6363.

[28] M. A. Boles, D. Ling, T. Hyeon, D. V. Talapin, *Nat. Mater.* **2016**, *15*, 141.

[29] D. Zhitomirsky, O. Voznyy, L. Levina, S. Hoogland, K. W. Kemp, A. H. Ip, S. M. Thon, E. H. Sargent, *Nat. Commun.* **2014**, *5*, 3803.

[30] G. H. Carey, I. J. Kramer, P. Kanjanaboos, G. Moreno-Bautista, O. Voznyy, L. Rollny, J. A. Tang, S. Hoogland, E. H. Sargent, *ACS Nano* **2014**, *8*, 11763.

[31] D. M. Balazs, D. N. Dirin, H.-H. Fang, L. Protesescu, G. H. ten Brink, B. J. Kooi, M. V. Kovalenko, M. A. Loi, *ACS Nano* **2015**, *9*, 11951.

[32] W. Walravens, J. D. Roo, E. Drijvers, S. ten Brinck, E. Solano, J. Dendooven, C. Detavernier, I. Infante, Z. Hens, *ACS Nano* **2016**, *10*, 6861.

[33] S. John, C. Soukoulis, M. H. Cohen, E. N. Economou, *Phys. Rev. Lett.* **1986**, *57*, 1777.

[34] K. S. Jeong, J. Tang, H. Liu, J. Kim, A. W. Schaefer, K. Kemp, L. Levina, X. Wang, S. Hoogland, R. Debnath, L. Brzozowski, E. H. Sargent, J. B. Asbury, *ACS Nano* **2012**, *6*, 89.

[35] R. Wang, Y. Shang, P. Kanjanaboos, W. Zhou, Z. Ning, E. H. Sargent, *Energy Environ. Sci.* **2016**, *9*, 1130.

[36] A. G. Pattantyus-Abraham, I. J. Kramer, A. R. Barkhouse, X. Wang, G. Konstantatos, R. Debnath, L. Levina, I. Raabe, M. K. Nazeeruddin, M. Grätzel, E. H. Sargent, *ACS Nano* **2010**, *4*, 3374.

[37] D.-K. Ko, A. Maurano, S. K. Suh, D. Kim, G. W. Hwang, J. C. Grossman, V. Bulović, M. G. Bawendi, *ACS Nano* **2016**, *10*, 3382.

[38] X. Lan, O. Voznyy, A. Kiani, F. P. García de Arquer, A. S. Abbas, G. H. Kim, M. Liu, Z. Yang, G. Walters, J. Xu, M. Yuan, Z. Ning, F. Fan, P. Kanjanaboos, I. J. Kramer, D. Zhitomirsky, P. Lee, A. Perelgut, S. Hoogland, E. H. Sargent, *Adv. Mater.* **2016**, *28*, 299.

[39] X. Lan, O. Voznyy, F. P. García de Arquer, M. Liu, J. Xu, A. H. Proppe, G. Walters, F. Fan, H. Tan, M. Liu, Z. Yang, S. Hoogland, E. H. Sargent, *Nano Lett.* **2016**, *16*, 4630.

[40] Z. Ning, H. Dong, Q. Zhang, O. Voznyy, E. H. Sargent. *ACS Nano* **2014**, *8*, 10321.

[41] Z. Yang, A. Janmohamed, X. Lan, F. P. García de Arquer, O. Voznyy, E. Yassitepe, G.-H. Kim, Z. Ning, X. Gong, R. Comin, E. H. Sargent, *Nano Lett.* **2015**, *15*, 7539.

[42] J. J. Peterson, T. D. Krauss, *Nano Lett.* **2006**, *6*, 510.

[43] S. Pradhan, A. Stavrinadis, S. Gupta, Y. Bi, F. Di Stasio, G. Konstantatos, *Small* **2017**, *13*, 1700598.

[44] C. J. Hages, N. J. Carter, R. Agrawal, *J. Appl. Phys.* **2016**, *119*, 014505.